Available online at www.sciencedirect.com
SCIENCE DIRECT
Talanta 69 (2006) 435–442
Talanta
www.elsevier.com/locate/talanta

Electrodeposited sol–gel-imprinted sensing film for cytidine recognition on Au-electrode surface

Zhaohui Zhang, Lihua Nie, Shouzhuo Yao *

State Key Laboratory of Chem/Biosensing and Chemometrics, College of Chemistry and Chemical Engineering, Hunan University, Changsha 410082, China

Received 25 July 2005; received in revised form 4 October 2005; accepted 5 October 2005
Available online 7 November 2005

Abstract

A novel thin molecularly imprinted sol–gel film with specific recognition for cytidine was electrodeposited on the surface of piezoelectric quartz crystal (PQC) Au-electrode. In this method, a sufficiently negative potential was applied to the electrode surface to generate hydroxyl ions, which play the role of the catalyst for the hydrolysis and condensation of 3-(aminopropyl)trimethoxysilane (APTMS). The process of the preparation of the imprinted sol–gel film was investigated in detail by using the piezoelectric quartz crystal impedance (PQCI) technique and cyclic voltammetry. The thickness of the imprinted film was controlled easily by adjusting the applied potential and the deposited time. The binding capacity and the selectivity of the electrodeposited imprinted sol–gel film were also studied in detail by using PQCI, electrochemically impedance technique and capacitance technique. The electrodeposited imprinted sol–gel film exhibited high selectivity toward cytidine in comparison to interfering substances. The dissociation constant (K_d) in the nanomolar range indicated a strong imprinted interaction existing between the electrodeposited sol–gel-imprinted film and the template cytidine.

Keywords: Molecularly imprinted; Sol–gel; Cytidine recognition; Electrodeposited

1. Introduction

Applications of molecularly imprinted polymers (MIPs) for sensing materials attract growing interest for their potential merits, such as good mechanical strength, durability to heat and pressure, physical robustness, high affinity and outstanding substrate recognition ability [1–5]. Many methods for synthesis have been developed, such as precipitation polymerization [6], electrosynthesis polymerization [7], surface imprinting polymerization [8], and scaffold imprinting polymerization [9] and so on. Among these methods, the recently developed self-assembly molecularly imprinting polymerization based on sol–gel technique is one of the fastest emerging fields [10,11].

Sol–gel approach has been employed to develop new materials for chemical sensors, separations, optical media, and solid-state electrochemical devices because the sol–gel-derived materials can yield high sensitivity and long-term stability [12–15]. The most common configurations of sol–gel-derived materials are monoliths and thin films. Generally, monoliths are prepared by pouring the silica sol into a container and allowing it to gel, age, and dry slowly. Thin films of silica have been prepared by dip-coating or spin-coating the silica sol on the surface of a suitable substrate. Few years ago, the fabrication of sol–gel-derived hydrophobic silica films using an electrodeposition procedure was reported [16,17]. However, the film usually flakes off the Au-electrode surface, which is an extensively applied substrate for the analytical research, especially in the piezoelectric quartz crystal (PQC) MIPs sensor. Thus, it is necessary to improve the sol–gel technique to promote the sol–gel film adhesion to the surface stably.

In this work, a novel sol–gel-imprinted film stably deposited on the surface of the PQC Au-electrode by using the self-assembly and electrodeposited technique was achieved. 1,6-hexanedithiol and Au nanoparticles were introduced during the preparation to avoid the resultant electrodeposited sol–gel film flaking off. A significantly negative potential was applied to increase the pH near Au-electrode surface, which resulted in a homogeneous thin sol–gel cytidine imprinted film on the Au-

* Corresponding author.
E-mail address: szyao@hnu.net.cn (S. Yao).

0039-9140/$ – see front matter © 2005 Elsevier B.V. All rights reserved.
doi:10.1016/j.talanta.2005.10.008

electrode surface steadily. 3-(Aminopropyl)trimethoxysilane (APTMS) was proposed as the silicon precursor. The deposition condition was investigated in detail. The characteristics of the sol–gel-imprinted PQC Au-electrode during the self-assembly and electrodeposition were investigated by using piezoelectric technique and cyclic voltammetry. The binding performance of the sol–gel cytidine imprinted electrodeposited film was also discussed by using the piezoelectric quartz crystal impedance (PQCI) technique, electrochemical impedance technique and capacitance technique. The results show that this sol–gel electrodeposition method is a feasible method for the preparation of imprinted sensing film.

2. Experimental section

2.1. Reagents

Guanosine, adenosine, cytidine, thymidine, uridine, deoxythymidine, deoxyguanosine, and adenosine monophosphate (AMP) were purchased from Sigma Chemical Co. 1,6-Hexanedithiol, hydrogen tetrachloroaurate(III) ($HAuCl_4.4H_2O$), and APTMS (97%) were purchased from Aldrich. Anhydrous ethanol, sodium hydroxyl, potassium ferricyanide, potassium ferrocyanide, potassium di-hydrogen phosphate, and di-sodium hydrogen phosphate were purchased from Changsha Chemical Co. Phosphate buffer solution (0.1 M, formed by mixing KH_2PO_4 with Na_2HPO_4 solutions, PBS) was used as background solution.

2.2. Apparatus

9 MHz PQC (AT-cut, 12.5 mm in diameter) coated with Au electrode (6 mm in diameter) on both sides was used. The experimental setup for PQCI can be found in our previous work [18]. The conductance (G) and susceptance (B) of the PQC Au electrode were measured synchronously with a HP 4192A LF impedance analyzer (frequency range 5 Hz–13 MHz, USA). Application program was written in Visual Basic (VB 5.0) to control the HP 4192A LF impedance analyzer. The resonant frequencies, equivalent parameters, data-collecting time, and scan times were recorded during the experiments.

An electrochemical workstation (CHI660A, Shanghai Chenhua Instrument Co.) was employed to investigate the electrochemical performance of the sol–gel-imprinted electrodeposited film. All electrochemical experiments were performed using a three-electrode system with the sol–gel-imprinted Au-electrode as the working electrode, a platinum electrode as the auxiliary electrode, and a saturated calomel electrode (SCE) as reference electrode.

2.3. Preparation of the sol–gel film

The preparation of Au nanoparticles was carried out according to a previously reported work [19]. 1.8 ml of 1% (w/w) sodium citrate solution was added into 50 ml of 0.01% (w/w) $HAuCl_4$ boiling solution, refluxed for ca.15 min until a wine-red color solution was observed and cooled at room temperature. The size of the resultant Au nanoparticles was ca.10–20 nm by using scanning electron microscopy.

As shown in Fig. 1, prior to electrodeposition, the surface of the PQC Au-electrode was modified with organic/inorganic multilayer by using the self-assembly technique. Firstly, the Au-electrode was immersed in an ethanol solution of 1,6-hexanedithiol (0.01 M) for 12 h, rinsed with ethanol and dried under nitrogen gas. Secondly, Au nanoparticles were adsorbed on the surface of the Au-electrode via covalent bond between Au and thiol, which was achieved by immersing the Au-electrode into Au nanoparticles colloid for 6 h. Thirdly, the electrode was immersed in toluene solution of 0.1 M APTMS for 12 h to accomplish the layer-by-layer self-assembly procedure.

The electrodeposited sol–gel film on the surface of the self-assembled PQC Au-electrode was carried out by using cyclic voltammetry. A solution containing 2.0 ml of 0.2 M KCl, 2.0 ml of ethanol, and 0.5 ml of APTMS, was sonicated for ca. 3 min until a homogeneous phase (initial sol) was observed. About 200 μl of 0.1 M cytidine solution was added into 2 ml of the initial sol and stirred. Then negative potential from −0.4 to −1.2 V (versus SCE, the scanning rate is 0.05 mV/s) was applied to the self-assembled PQC Au-electrode for 20–30 min. Finally, the electrodeposited sol–gel-imprinted Au-electrode was taken out of the cell, rinsed with ethanol and dried in a desiccator at room temperature for 24 h. The electrodeposited non-imprinted sol–gel Au-electrode was prepared with the same procedure without addition of cytidine into the initial sol.

The extraction of the template molecule from the imprinted sol–gel film was achieved through repeatedly washing the imprinted sol–gel electrode with the ethanol and double-distilled water until the template molecule could no longer be detected under UV (λ_{max} = 280 nm) from the supernatant.

2.4. PQCI measurements

In the following step, the variations of the equivalent parameters (the response frequency; the motional resistance and the static capacitance) were real-time recorded with HP 4192A impedance analyzer. After the sol–gel PQC Au-electrode was immersed in 10 ml of background solution (0.1 M PBS, pH 7.0) for 20 min, stable base-line parameters were obtained. Then a series of sample solutions (cytidine standard solutions) were added into the background solution in an increasing concentration order and the corresponding response parameters were recorded. After the measurement, the electrode was immersed in ethanol and double-distilled water to remove the adsorbed analyte.

2.5. Electrochemical measurements

The electrochemical impedance measurements were performed in the presence of 10 ml of 10 mM $K_3[Fe(CN)_6]/K_4[Fe(CN)_6]$ (1:1) PBS (containing 0.2 M NaCl solution as supporting electrolyte). Prior to addition of sample into the background solution, the three electrodes were stabilized in the background solution for ca. 20 min. The sample was added in an increasing concentration order and the time interval for the addi-

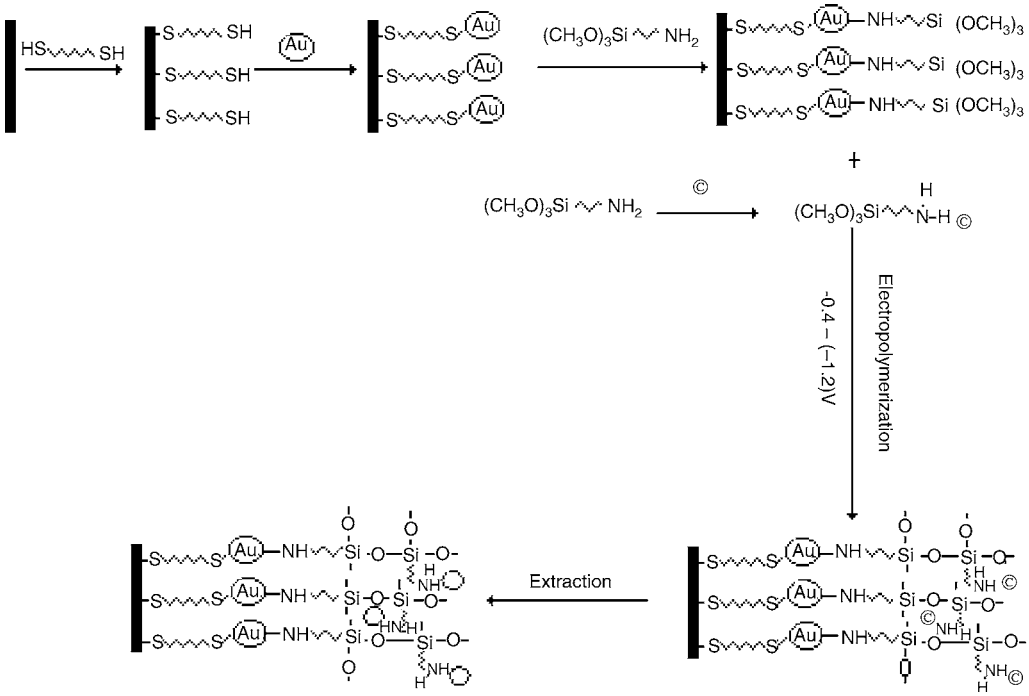

Fig. 1. Schematic representation of the preparation of molecularly imprinted film on the surface of PQC Au-electrode. HS SH corresponds to 1,6-hexanedithiol; Au to Au nanoparticles; $(CH_3O)_3Si$ NH_2 to APTMS and © to cytidine.

tion of the standard sample solution was 15 min. The temperature of the tested solution in electrochemical cell was controlled at $25 \pm 0.1\,^{\circ}C$. After the measurement, the analyte was removed as mentioned above.

3. Result and discussion

3.1. Imprinting procedure

A cytidine imprinted sol–gel film attempted to deposit directly on the surface of the PQC Au-electrode without adding acid-catalyzer or base-catalyzer into the sol. In order to achieve it, a significantly negative potential was applied to increase the pH at the electrode surface. The concentration increase of hydroxyl ions, which act as a catalyst in the condensation process, resulted in the deposition of a sol–gel film. The reactions taking place in the two-step procedure are as follows:

$$NH_2(CH_2)_3Si(OCH_3)_3 + 3H_2O \rightarrow NH_2(CH_2)_3Si(OH)_3 + 3CH_3OH \quad (1)$$

$$NH_2(CH_2)_3Si(OH)_3 + NH_2(CH_2)_3Si(OH)_3 \rightarrow NH_2(CH_2)_3(OH)_2Si{-}O{-}Si(OH)_2(CH_2)_3NH_2 + H_2O \quad (2)$$

Previous studies showed that it was very difficult to form a thin, stable sol–gel film on the surface of Au-electrode [16], which is an extensively applied substrate for the analytical research, especially in the PQC-MIP sensor. In order to solve this problem, firstly, we attempted to assemble a layer of organic silicate reagent by using (3-mercaptopropy1)triethoxysilane, which bifunctional organics (thiol) have two reactive centers, one reacts with an oxide and the other reacts with a metal for attachment of a strongly adherent thin silica layer on Au surfaces [20]. However, the insulation of the resulted modified layer made the further electrodeposition of alkoxysilane on the electrode impossible. Therefore, a hybrid multilayer film based on thiol-Au nanoparticles and Au nanoparticles-amidogen has been fabricated via self-assembly because a compact film of Au nanoparticles has good conductivity [21]. The procedure is shown in Fig. 1. For each process, the mass modified on the surface of the PQC Au-electrode was calculated by using the piezoelectric technique and the results are given in Table 1. Given the thiol has a strong tendency to adsorb onto Au surface, it is reasonable to assume that all the Au nanoparticles are linked with the APTMS molecules. Thus, the value of 1.3 of the molar ratio between the adsorbed Au nanoparticles and the adsorbed APTMS suggests the combinations between the Au nanoparticle and APTMS may be in molar ratio of 1:1, and may be in that of 2:1 or more.

Table 1
The mass change on the surface of PQC during the self-assembly

Modification procedure	Frequency shift (Hz)	Mass change (ng)
1,6-Hexanedithiol	261.4 ± 0.6	405.1 ± 0.9
Au nanoparticles	205.7 ± 0.4	318.8 ± 0.6
APTMS	184.5 ± 0.3	290.0 ± 0.5
Electrodeposition		
10[a]	623.2 ± 0.3	966.0 ± 0.5
20[a]	1131.3 ± 0.2	1753.5 ± 0.4
30[a]	1325.2 ± 0.5	2054.1 ± 0.8
40[a]	1554.7 ± 0.1	2409.8 ± 0.3

[a] Number of scanning cycle.

In order to investigate further the change of the conductance of the PQC Au-electrode during the assembly, cyclic voltammetry was employed. When 1,6-hexanedithiol was modified on the surface of the PQC, the significant lack of faradic current than that of the bare Au-electrode was observed, which indicates that the film is compact and electrons hardly permeate it. It is important to note that the introduction of Au nanoparticles resulted in the increment of the redox peak of the PQC Au-electrode, which manifested that Au nanoparticles were not only self-assembled on the electrode surface, but also partly distributed within the film as tiny conduction centers and facilitated the electron-transfer. Although the faradic current of the Au-electrode decreased again when APTMS was adsorbed on the surface of the PQC, the PQC Au-electrode was still electric because a pair of tiny redox peaks was observed. Thus, it made the further electrodeposition possible.

The electrodeposition process can be performed in many ways. Cyclic voltammetry, a classical and conventional method, was employed in this work. A reduction wave commencing at potential more negative than −0.8 V was observed due to the reduction of oxygen to hydroxyl ions at the Au electrode surface [16]. The current of the reduction wave reduced with the increment of the cyclic scan, which can be explained by the poor conductance and compactness of the resultant imprinted sol–gel film. When the scanning cycle was over 40, the reduction wave almost disappeared and did not reduce with the increment of the scanning cycle for the insulation of the resultant sol–gel film. This indicated that the thickness of the electrodeposition film did not increase any more. A layer of imprinted sol–gel film was deposited steadily on the PQC Au-electrode surface by using scanning electron microscope technique.

Among the influencing factors of the film thickness, the applied potential was the most important. The more negative the applied potential, the more the thickness of the resultant sol–gel film. For example, the thickness of the film obtained by applying the potential over the range −0.4 to −1.0 V for 40 cyclic scans was calculated as 40.7 nm. However, when the applied potential was over the range −0.4 to −1.2 V, the thickness of the resultant film was 90.1 nm. Another parameter influencing the deposited film thickness was the deposition time. For example, by applying −1.2 V for 40 cyclic scans, the resultant film's thickness was 1.85 times thicker than that of 20 cyclic scans by applying the same potential.

3.2. Performance of the sol–gel-imprinted film

After removal of the template molecule from the imprinted film, imprinted cavities were obtained. The binding of the sol–gel-imprinted film with template molecule just depended on these resultant imprinted cavities. In piezoelectric analysis, the Sauerbrey equation shows only the mass effect on the frequency change of the quartz crystal as follows [22]:

$$\Delta f_0 = -\frac{2f^2\Delta m}{(\rho_q\mu_q)^{1/2}A} \quad (3)$$

where f is the fundamental frequency; A the geometric surface area; ρ_q and μ_q are the density and shear modulus of quartz, respectively. Additionally, the physical and chemical properties of the background liquid also cause the frequency to change. The effect of the density (ρ_L) and viscosity (η_L) of the liquid on the resonant frequency is as follows [23]:

$$\Delta f_0 = -\frac{f^{3/2}(\rho_L\eta_L)^{1/2}}{(\pi\rho_q\mu_q)^{1/2}} \quad (4)$$

The relationship between the motional resistance (R_m) and the ($\rho_L\eta_L$) of the liquid is given as follows [24]:

$$R_m = \frac{(2\pi f_0\rho_L\eta_L)^{1/2}A}{\kappa^2} \quad (5)$$

where κ is the electromechanical coupling factor. The absolute value $\Delta f_0/\Delta R_m$ for the net density/viscosity effect on the 9 MHz PQC resonance is approximately 10.1 Hz/Ω [25]. Obviously, the larger the absolute value of $\Delta f_0/\Delta R_m$, the weaker the viscous effect and the stronger the mass effect.

As given in Fig. 2, when a sample solution (cytidine standard solution) was added, the response frequency (Δf_0) reduced with the increment of time and then reached a stable value. Simultaneously, the change of motional resistance (ΔR_m) and static capacitance (ΔC_0, which is relative to the capacity and structure of the electrical double layer) increased. The absolute value of $\Delta f_0/\Delta R_m$ (62.5 Hz/Ω) is higher than that of the characteristic absolute value of $\Delta f_0/\Delta R_m$ (10.1 Hz/Ω) [25]. This indicates that the frequency decrease is a result of the synergistic effect from the mass factor. Hence, a series of standard sample solutions in an increasing concentration order were added, and the response frequencies of the sol–gel sensor were recorded. As given in Fig. 3, the response frequencies of the imprinted sol–gel sensor to the analyte were more significant than that of the non-imprinted sol–gel sensor. This can be attributed to the much more binding sites existing in the imprinted sol–gel film than that in the non-imprinted sol–gel film. The frequency shift increased with

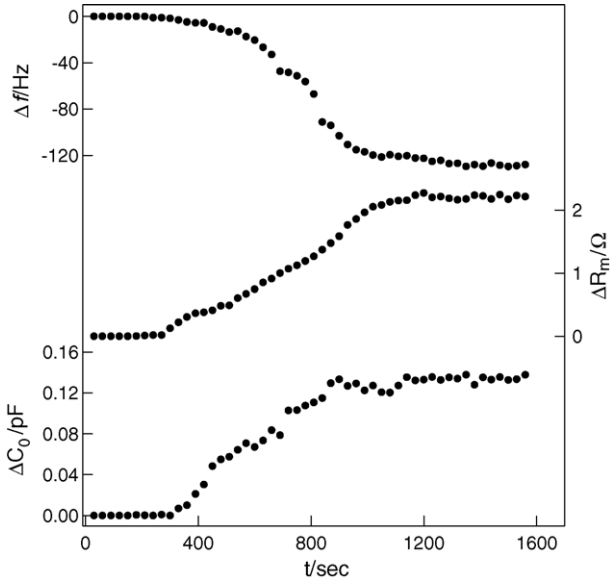

Fig. 2. Typical PQCI spectrum of the sol–gel-imprinted PQC sensor for the sample solution (sample concentration 2.5×10^{-7} M).

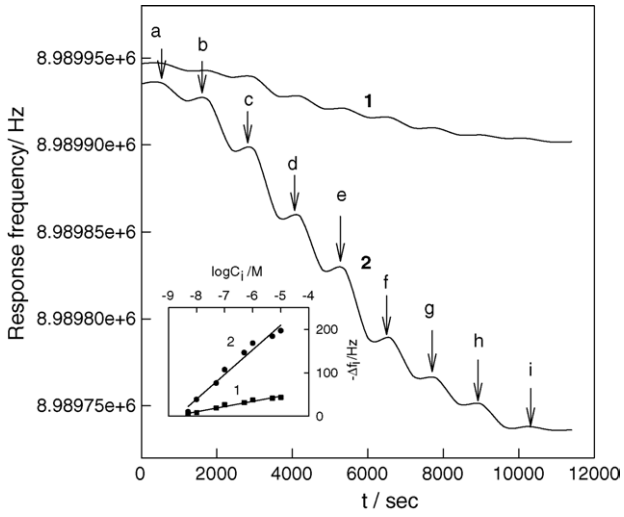

Fig. 3. Response course of the frequency shift of the sensor to each concentration of cytidine. (1) Non-imprinted film. (2) Imprinted film. (a) 5×10^{-9} M; (b) 1×10^{-8} M; (c) 5×10^{-8} M; (d) 1×10^{-7} M; (e) 5×10^{-7} M; (f) 1×10^{-6} M; (g) 5×10^{-6} M; (h) 1×10^{-5} M. (i) 5×10^{-5} M.

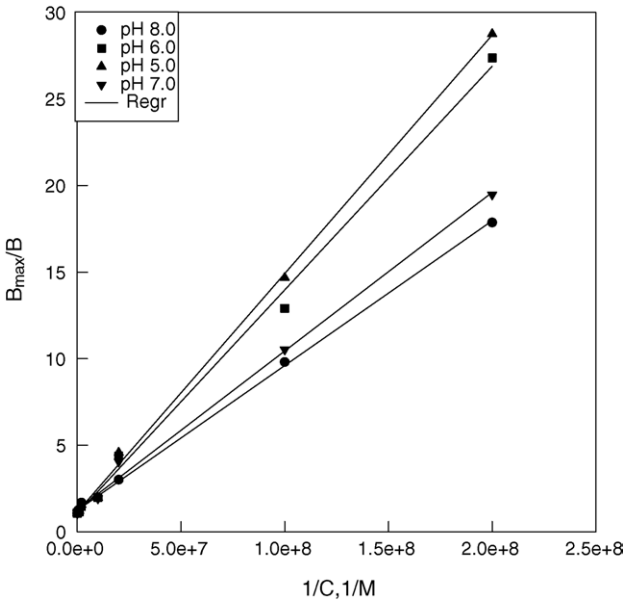

Fig. 4. Specific binding performance of the imprinted sol–gel film in buffer solutions with different pHs. Data were plotted as bound max/bound (B_{max}/B) vs. 1/concentration. K_ds were calculated from the slope of the curves.

the increment of the sample concentration over a concentration range from 5.0×10^{-9} M to 5.0×10^{-5} M. However, when the sample concentration was over 5.0×10^{-5} M, the frequency shift did not increase any more. The reason may be that the imprinted binding amount of the imprinted sol–gel film toward the template nucleotide is limited due to the limited imprinted sites existing in the imprinted film. As in our previous work [26], a relationship between the frequency shift (Δf_i, Hz) and the sample concentration (C_i, M) was regressed as follows:

$$-\Delta f_i = 494.2 + 56.9 \log C_i, \qquad r = 0.97 \tag{6}$$

In this work, the binding capacity of the sol–gel-imprinted film was further investigated in different pH PBS by using piezoelectric technique. The binding capacities of the imprinted film to template molecule at pH 5.0, 6.0, 7.0, 8.0 were measured, respectively. From Fig. 4, the affinity of the imprinted film to template was estimated for each buffer solution and the values of the dissociation constants (K_d) were estimated. As shown in Table 2, all K_d are in the nanomolar range. This suggests a strong imprinted film-template interaction existing between the imprinted film and the nucleotide [27]. For non-imprinted sol–gel film, K_d values vary from 1.05 μM at pH 5.0 to 1.08 μM at pH 8.0, no significant effect of pH on the binding capacity of it with cytidine was observed. However, for imprinted sol–gel film, K_d value at pH 5.0 (0.19) is twice over that at pH 8.0 (0.084), which indicates its enhanced affinity at high pH. By comparing non-imprinted sol–gel film and imprinted sol–gel film, the optimum binding pH was estimated to be between pH 7.0 and 8.0, where the affinity of the imprinted sol–gel film was several times higher than that of the non-imprinted sol–gel film.

Table 2
Influence of pH on cytidine binding of sol–gel film

pH	K_d (μM)	
	Imprinted film	Non-imprinted film
5.0	0.19	1.05
6.0	0.14	0.99
7.0	0.13	1.2
8.0	0.084	1.08

Studies showed that the swelling of the imprinted polymer upon the association of the analyte enhances the permeability of the electrolyte through the imprinted polymer film [2,26]. Thus, it is possible to investigate the binding performance of the sol–gel-imprinted film with cytidine by using the electrochemical impedance technique, which is an effective method to probe the features of surface-modified electrodes [28]. Generally, a typical shape of an electrochemical impedance spectrum (Nyquist plot) includes a semicircle segment, observed at higher frequencies, which corresponds to the electron-transfer resistance of the modified film on Au-electrode surface (R_{et}). As given in Fig. 5, the sample concentration ranging from 1×10^{-6} to 5×10^{-4} M, R_{et} reduced with the increment of the sample concentration. However, when the sample concentration was lower than 1×10^{-6} M, the electrochemical impedance spectrum did not give significant change. According to previous studies [29], it was found that the imprinted adsorption data fit well to the Freundlich isotherm model. Therefore, the lower the sample concentration, the smaller the adsorbed mass. Thus, when the adsorbed mass was too small, the swelling degree of the imprinted film was also too small to generate significant change in the electrochemical impedance. However, when the sample concentration was over 5×10^{-4} M, no significant change of the electron-transfer resistance (R_{et}) was also observed. It is interesting to note that a linear relationship between the circular diameter of the electrochemical impedance spectra ($\log R_{et}$, kΩ) and the sample concentration ($\log C_i$, M) ranging from

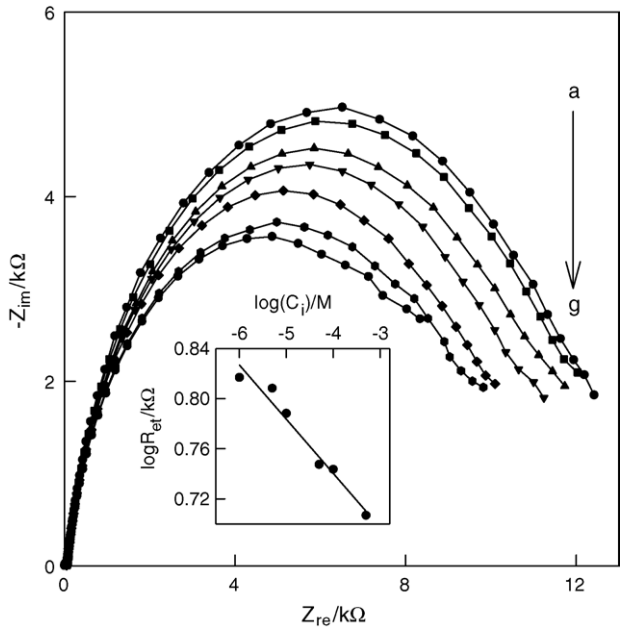

Fig. 5. Nyquist plot of electrochemical impedance spectra of the sol–gel-imprinted PQC Au-electrode upon interaction with cytidine of different concentrations. (a) 0 M. (b) 1×10^{-6} M. (c) 5×10^{-6} M. (d) 1×10^{-5} M. (e) 5×10^{-5} M. (f) 1×10^{-4} M and (g) 5×10^{-4} M. Inset: relationship between the circular diameter and the cytidine concentration.

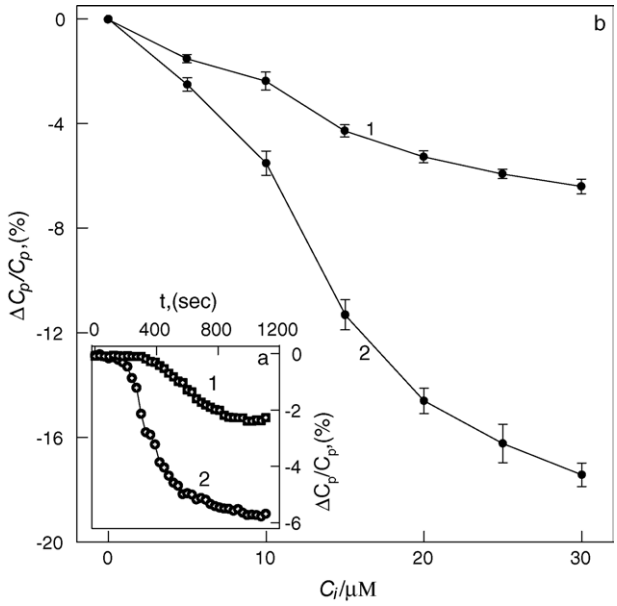

Fig. 6. Capacitance shift as a function of the concentration of cytidine. Inset: real-time binding curves of sol–gel film with cytidine (10 μM) by using the capacitive sensing technique. (1) Non-imprinted sol–gel film. (2) Imprinted sol–gel film.

1×10^{-6} M to 5×10^{-4} M was observed (Inset in Fig. 5) and regressed as follows:

$$\log R_{et} = 0.567 - 0.043 \log C_i, \qquad r = 0.97 \tag{7}$$

This indicated that the electrochemical impedance technique is a feasible method for quantified analysis of the sample concentration.

An attempt was made to characterize the binding performance of the film to the template molecule by using the capacitance technique because the resultant electrodeposited sol–gel imprinted film is insulating. According to previous studies [30,31], when one plate is covered with an insulator and the other is an image electrode of insulator/electrolyte solution interface connected to the counter electrode, if the resultant phase angle (θ) is close to 90°, the device displays near-ideal capacitor behavior. In this work, when the frequency of 1000 Hz was chosen as the work frequency, the resultant phase angle (θ) was 85.5°. This indicated it is possible to investigate the binding performance of the sol–gel sensor toward the template molecule by using capacitance technique.

According to previous studies [30,31], the capacitance, C, between two parallel plates separated with a distance d is given by equation:

$$C = \frac{\varepsilon_0 \varepsilon A}{d} \tag{8}$$

where ε_0 is the permittivity of free space; ε the dielectric constant of the material between the plates, and A is the surface area. Using capacitive method, the real-time combination curves of imprinted/non-imprinted sol–gel film with template molecule are shown in Fig. 6(a). When a sample was added into the background solution, the capacitance of the imprinted sol–gel film reduced for ca.10 min and then became stable. The change of the sensor capacitive response with the cytidine concentration is shown in Fig. 6(b). The results demonstrated when the concentration exceeds 30 μM; there is no obvious capacitance change. The total signal change caused by cytidine for imprinted sol–gel sensor was more than 17%. For non-imprinted sol–gel sensor, the total signal change was only ca. 6.0%. The results confirm that in the case of the sensor for cytidine, the analyte binding with the film is essential for the changes in capacitance.

3.3. Selectivity and stability

The key property of the molecularly imprinted sensor is its capability of recognizing a specific target molecule. The selective recognition is based on functional group and shape complementarity between the template molecules and 3D structure of binding sites in the imprinted film. To assess the recognition performance of the electrodeposited imprinted sol–gel film, selectivity factor (κ_{it}), which is defined as the ratio of the sensor's frequency shift toward the interfering substance to that toward the template molecule, was calculated. A series of interfering compounds, which concentrations were 5×10^{-5} M, were tested by using piezoelectric technique. As shown in Table 3, all K_{it}s of the imprinted sol–gel sensor to interfering substances are much smaller than that of the non-imprinted sol–gel sensor, which suggested that the imprinted sol–gel sensor can distinguish cytidine from the interfering substances.

Since different R_{et} can be obtained for the sol–gel-imprinted Au-electrode before and after its interaction with the analyte, the electrochemical impedance technique could also serve as a tool to evaluate selectivity of the imprinted film modified Au-electrode. As mentioned above, a series of interfering substances

Table 3
The selectivity of the imprinted sol–gel film

Interfering substance	Imprinted sol–gel film		Non-imprinted sol–gel film	
	$K_{it} = \Delta f_i/\Delta f_t$ [a]	$K_{it} = \Delta R_{et(i)}/\Delta R_{et\ (t)}$ [b]	$K_{it} = \Delta f_i/\Delta f_t$ [a]	$K_{it} = \Delta R_{et(i)}/\Delta R_{et(t)}$ [b]
Guanosine	0.21	0.24	0.93	1.01
Thymidine	0.36	0.34	0.91	0.96
Uridine	0.44	0.41	0.89	0.99
Deoxythymidine	0.38	0.31	0.95	0.94
Deoxyguanosine	0.20	0.23	0.90	0.95
Adenosine	0.18	0.25	1.08	0.97
AMP	0.13	0.20	0.95	0.99

[a] K_{it} is defined as the ratio of the sensor's frequency shift toward the interfering substance to that toward the template molecule.
[b] K_{it} is defined as the ratio of the change of the diameter of the electrochemical impedance spectra toward the interfering substance to that toward the template molecule.

were also tested and the results are also shown in Table 3. Similar results of the electrochemical impedance experiment with that of the piezoelectric technique were observed, which further proved that the imprinted sol–gel film can selectively recognize cytidine from the interfering substances. In both cases, special selectivity of the imprinted film toward its template is demonstrated. The shape effect seems to play a crucial role in the selectivity of the imprinted film. For example, uridine, which has very similar size to cytidine, its selectivity factor (K_{it}) is greater than other interfering substance. However, no significant difference in the selectivity factor (K_{it}) between guanosine and deoxyguanosine; thymidine and deoxythymidine were observed.

Another important property of the imprinted PQC sensor is its stability. For an imprinted sol–gel sensor, with membrane thickness of ca. 100 nm, repeatedly regenerated (seven times), the binding capacity of the imprinted film with the template molecule was measured during 4 weeks and the result was found to decrease $14 \pm 3\%$ of its original binding capacity. The affinity decrease may be caused by the partial destruction of the imprinted binding sites when the template molecule was washed out from the imprinted film.

4. Conclusions

A novel cytidine imprinted sol–gel silicate film was electrodeposited on the Au-electrode surface by using a significantly negative potential to provide hydroxide ions, which play the role of catalyst in the hydrolysis and condensation of APTMS in this work. Prior to electrodeposition, the surface of the Au-electrode was modified with organic/inorganic multilayer via self-assembly. The introduction of Au nanoparticles can avoid the film flaking off. The measured K_ds in nanomolar indicated a strong binding interaction between the electrodeposited sol–gel-imprinted film and cytidine. The investigation of performance of the electrodeposited sol–gel-imprinted sensor by using piezoelectric technique, electrochemical impedance technique and capacitance technique indicated: (1) the piezoelectric technique can give the widest response concentration range (5.0×10^{-9} to 5.0×10^{-5} M); (2) electrochemical impedance detection is proved to be a convenient and sensitive method for studying the imprinted sol–gel film; even the imprinted film may swell upon association with the template molecule; (3) among the tested techniques, the capacitance technique gives the narrowest response range (5–30 μM), but it provides an alternative detection tool for an insulated imprinted sol–gel film and its binding with template. All these results suggest that the electrodeposited sol–gel imprinted method is feasible.

Acknowledgements

We gratefully acknowledge support of this work by the National Natural Science Foundation (No. 20335020) and the Research Fund for the Doctoral Program of Higher Education (No. 20030532017).

References

[1] J. Matsui, K. Akamatsu, S. Nishiguchi, D. Miyoshi, H. Nawafune, K. Tamaki, N. Sugimoto, Anal. Chem. 76 (2004) 1310–1315.
[2] N. Sallacan, M. Zayats, T. Bourenko, A.-B. Kharitonov, I. Willner, Anal. Chem. 74 (2002) 702–712.
[3] K. Haupt, K. Mosbach, Chem. Rev. 100 (2000) 2495–2504.
[4] C. Baggiani, L. Anfossi, C. Giovannoli, C. Tozzi, Talanta 62 (2004) 1029–1034.
[5] H.S. Ji, S. McNiven, K. Ikebukuro, I. Karube, Anal. Chim. Acta 390 (1999) 93–100.
[6] S. Marx, A. Zaltsman, I. Turyan, D. Mandler, Anal. Chem. 76 (2004) 120–126.
[7] H.H. Yang, S.Q. Zhang, W. Yang, X.L. Chen, Z.X. Zhuang, J.G. Xu, X.R. Wang, J. Am. Chem. Soc. 126 (2004) 4054–4055.
[8] L. Schweitz, Anal. Chem. 74 (2002) 1192–1196.
[9] S. Chia, J. Urano, F. Tamanoi, B. Dunn, J.-I. Zink, J. Am. Chem. Soc. 122 (2000) 6488–6489.
[10] J.B. Jia, B.Q. Wang, A.G. Wu, G.J. Cheng, Z. Li, S.J. Dong, Anal. Chem. 74 (2002) 2217–2223.
[11] J. Brunker, G. Scherer, Sol–Gel Science, Academic Press, New York, 1989.
[12] B.S. Ebarvia, S. Cabanilla, F. Sevilla, Talanta 66 (2005) 145–152.
[13] Y. Guo, L.A. Colón, Anal. Chem. 67 (1995) 2511–2516.
[14] D. Levy, Chem. Mater. 9 (1997) 2666–2670.
[15] F.L. Dickert, O. Hayden, Anal. Chem. 74 (2002) 1302–1306.
[16] P.N. Deepa, M. Kanungo, G. Claycomb, P.M.A. Sherwood, M.M. Collinson, Anal. Chem. 75 (2003) 5399–5405.
[17] B.R. Shacham, D. Avnir, D. Mandler, Adv. Mater. 11 (1999) 384–388.
[18] Y.A. Mao, W.Z. Wei, D.L. He, L.H. Nie, S.Z. Yao, Anal. Biochem. 306 (2002) 23–30.
[19] G. Frens, Nat. Phys. Sci. 241 (1973) 20.
[20] W.R. Thompson, T.E. Pemberton, Chem. Mater. 7 (1995) 130–136.
[21] Y. Liu, Y. Wang, R.-O. Claus, Chem. Phys. Lett. 298 (1998) 315–319.
[22] G. Sauerbrey, Z. Phyzik 155 (1959) 206–212.

[23] K.K. Kanazawa, J.G. Gordon, Anal. Chim. Acta 175 (1985) 99–105.
[24] H. Muramatsu, E. Tamiya, I. Karube, Anal. Chem. 60 (1988) 2142–2146.
[25] Q.J. Xie, Y.Y. Zhang, Y. Yuan, Y.H. Guo, X.J. Wang, S.Z. Yao, J. Electroanal. Chem. 484 (2000) 41–54.
[26] Z.H. Zhang, H.P. Liao, H. Li, L.H. Nie, S.Z. Yao, Anal. Biochem. 336 (2005) 108–116.
[27] A. Bossi, S.A. Piletsky, E.V. Piletska, P.G. Righetti, A.P.F. Turner, Anal. Chem. 73 (2001) 5281–5286.
[28] F. Patolsky, B. Filanovsky, E. Katz, I. Willner, J. Phys. Chem. B 102 (1998) 10359–10367.
[29] P. Sajonz, M. Kele, G.M. Zhong, B. Sellergren, G. Guiochon, J. Chromatogr. A 810 (1998) 1–17.
[30] H. Berney, J. West, E. Haefele, J. Alderman, W. Lane, J.-K. Collins, Sens. Actuators B 68 (2000) 100–108.
[31] Z.L. Cheng, E.K. Wang, X.R. Yang, Biosens. Bioelectron. 16 (2001) 179–185.